The Electrodynamics of a Pair of PV Modules with Connected Building Resistance

HIMANSHU DEHRA
American Institute-Industry Forum on Energy
1-140 Avenue Windsor, Lachine, Quebec H8R 1P7
CANADA

Abstract: - The electrodynamics of a pair of photovoltaic (PV) modules with connected resistance due to thermal mass of an outdoor room has been presented. The experiments were conducted on a pair of glass coated PV modules connected with a series electrical circuit through a rheostat. A steady state network model for a pair of PV modules connected with building resistive network has been proposed. The principles of electromagnetic wave theory have been applied to perform the energy balances on the discretised nodal elements in the network. The solution accuracy for prediction of temperatures at various nodes in the network is based on the magnitude and number of the connected resistances in the circuit, the smaller the shunt resistance value the greater has been the accuracy.

Key-Words: - PV module, rheostat, amplifier, conductance, network model

1 Introduction

The electrodynamics is movement of electrons by an applied electromagnetic force so as to cause transmission of heat and electricity through a conductor. The electrodynamics of a pair of photovoltaic (PV) modules has been investigated through a numerical and experimental study [1]. The glass coated photovoltaic modules were embedded in south façade of an outdoor room. The schematic of an outdoor room is illustrated in Fig. 1. The PV modules were connected in series electrical circuit through a 50 Ω rheostat [1]. The rheostat was a wire-wound coil with a sliding contact used to vary electrical resistance without interrupting the current and has another use in volume control of an amplifier. Electrical circuit for series connection of PV modules with a rheostat is illustrated in Fig. 2.

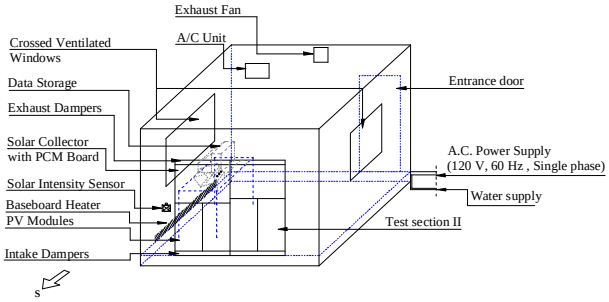

Fig. 1 Schematic of an outdoor room with test section for PV modules

The PV modules were adjoined through a wooden frame on the façade section of an outdoor room forming a parallel plate airflow passage with façade section. The useful heat transport into the room from PV modules has been achieved with an exhaust fan installed in an outdoor room. The façade section corresponding to PV modules was a polystyrene filled plywood board as an insulating back panel. The schematic of PV module test section with location of sensors is illustrated in Fig. 3.

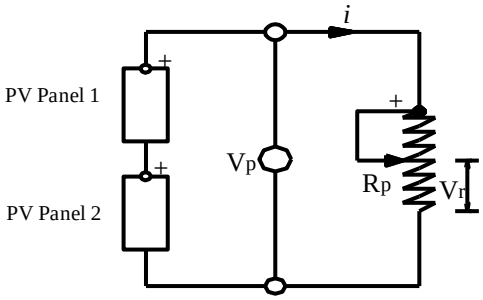

Fig. 2 Electrical circuit for PV modules with a rheostat

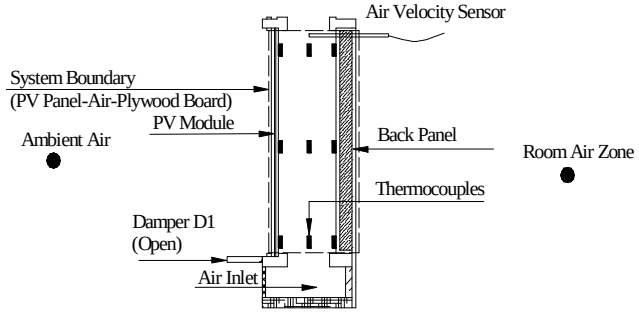

Fig. 3 Schematic of PV module test section with location of sensors

2 Problem Formulation

The network model for a pair of PV modules connected with building resistive network has been proposed. The assumptions applicable to network model are: (i) the electrical analog of thermal part of system boundary has been analysed as a parallel plate vertical channel; (ii) lumped temperatures at nodes; (iii) constant surface and air properties; (iv) negligible air heat conduction; (v) PV modules have negligible thermal storage in comparison to absorbed solar energy. The connected elements included in an integrated network circuit were discretised part resistances of a pair of PV modules, airflow passage and back panel. The system boundary of the electrical analog of thermal part of the network has been discretised into 10 resistive elements placed each on solid-air edges of PV module, back panel and center of air gap column.

2.1 Governing Equations

The governing equations representing heat conduction, heat exchange and heat transport in PV module test section are presented herewith [1]. The heat conduction equation for PV module is written as:

$$\frac{\partial^2}{\partial x^2} T_i + \frac{\partial^2}{\partial y^2} T_i + \frac{q_i}{k_i} = 0 \tag{1}$$

The heat conduction equation for insulating back panel is written as:

$$\frac{\partial^2}{\partial x^2} T_j + \frac{\partial^2}{\partial y^2} T_j = 0 \tag{2}$$

The boundary conditions for PV module and back panel facing airflow passage are written as:

$$-k_i \left(\frac{\partial}{\partial x} T_i\right) = hi_c \left(T_k - T_i\right) + \sum_{j=20}^{29} hi_{r_{i,j}} \left(T_j - T_i\right) \tag{3}$$

$$-k_j \left(\frac{\partial}{\partial x} T_j\right) = hj_c \left(T_k - T_j\right) + \sum_{i=0}^{9} hj_{r_{i,j}} \left(T_i - T_j\right) \tag{4}$$

The boundary condition representing energy balance between solid surface and air flowing through passage between PV module and back panel is given by:

$$m c_p \left(\frac{\partial}{\partial y} T_k\right) = hi_c W \left(T_i - T_k\right) + hj_c W \left(T_j - T_k\right) \tag{5}$$

The boundary condition for enthalpy change at inlet with respect to ambient air for first air node is:

$$H_a = m\, c_p \left(T_{10} - T_o\right) \tag{6}$$

Assuming no infiltration or air leakage sources in airflow passage between PV module and back panel, the continuity equation is satisfied is expressed as:

$$\rho_{air} A_c v_{mean} = \text{constant} \tag{7}$$

The governing equations (1-7) are applied to composite nodes in the network to perform finite difference approximations. The principles of electromagnetic wave theory have been applied to perform the energy balances on the discretised nodal elements in the network. The system of algebraic nodal equations for each of the node in the nodal network is henceforth established and solved using matrix inversion.

3 Problem Solution

The network has been solved with control volume finite difference method (CVFDM) with measured air velocity to calculate mass flow rate across one PV module [1]. The electromagnetic force due to solar irradiation has been assumed to be balanced with forces due to flow of electricity, vertical heat conduction, long wave heat radiation, heat convection, film heat transfer coefficients for an outdoor room and heat transport.

The energy balance equations for PV module, back panel and air nodes in the network are written as:

$$\Delta Q(amb)_{i,o} + \Delta Q(cond)_{i,i-1} + q \cdot \Delta V + ... \\ .... \Delta Q(conv)_{i,k} + \Delta Q(cond)_{i,i+1} + \sum_j Q(rad)_{i,j} = 0 \tag{8}$$

$$\Delta Q(zone)_{j,z} + \Delta Q(cond)_{j,j-1} + \Delta Q(conv)_{j,k} + ... \\ .... \Delta Q(cond)_{j,j+1} + \sum_i Q(rad)_{j,i} = 0 \tag{9}$$

$$\Delta Q(enth)_{k,k+1} + \Delta Q(conv)_{k,i} + \Delta Q(conv)_{k,j} = 0 \tag{10}$$

The matrix procedure is used for solution of unknown temperatures at the discretised nodes with constitution of network equations as per energy balances performed from Eqs. (8) to (10). The matrix equation for the composite nodes (1 to 30) of the network is written as [1]:

$$U_{30,30} \times T_{30,1} = Q_{1,30} \tag{11}$$

The resistances were assumed to be developed due to flow of heat and current in the circuit with incident steady state electromagnetic radiation of solar energy. The view factor algebra between composite surfaces of PV module and back panel has been derived with use of crossed-string method [1]. The model has been based on measured values of solar irradiation, electric power, air velocity,

ambient air and room air temperatures [1]. The schematic of network of distributed conjugate resistances of heat conduction, heat convection, heat radiation and heat transport is illustrated in Fig. 4.

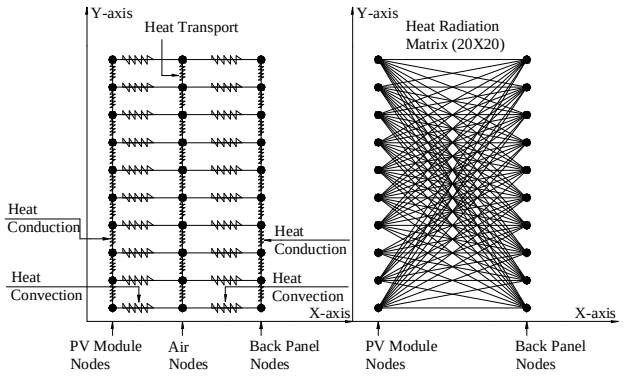

Fig. 4 Network of distributed conjugate resistances

3.1 Solution Procedure

The input values of ambient air temperature, room air temperature, solar intensity, air velocity at outlet and electric power from the experimental setup have been used to initialise the numerical solution [1]. The measured air velocity has used to obtain the mass flow rate for one PV module for calculating thermal capacity conductance terms for the air nodes. The thermal properties of PV module, air and back panel, are assumed to be constant except transmittance-absorbtance product of PV module, which has been calculated over a period of solar time for calculating absorbed solar radiation by PV module at the time of solar intensity measurement.

The non-linearity of temperature dependent boundary conditions has been eliminated by heat balance model [1]. The effect of radiation heat exchange between surface nodes of PV module and back panel has been considered in detail with radiosity-irradiation method assuming the enclosure analysis [1]. The radiation exchange factors have thus been evaluated using script factor matrix of size (20 X 20) [1].

The convection heat transfer coefficients are calculated using temperatures obtained from the heat balance model [1]. The conductance values are thus been obtained as per constitutive relations for heat conduction, heat convection, heat radiation and heat transport to formulate the U-matrix (30 X 30) after obtaining off-diagonal and diagonal entries [1]. The inverse of U-matrix (30 X 30) has been multiplied with the heat source element matrix (1 X 30), to obtain temperature matrix (30 X 1) for 30 nodes [1].

3.2 Results and Discussions

The temperature plots for PV module, air and back panel with volume of PV module test section are presented in Fig. 5.

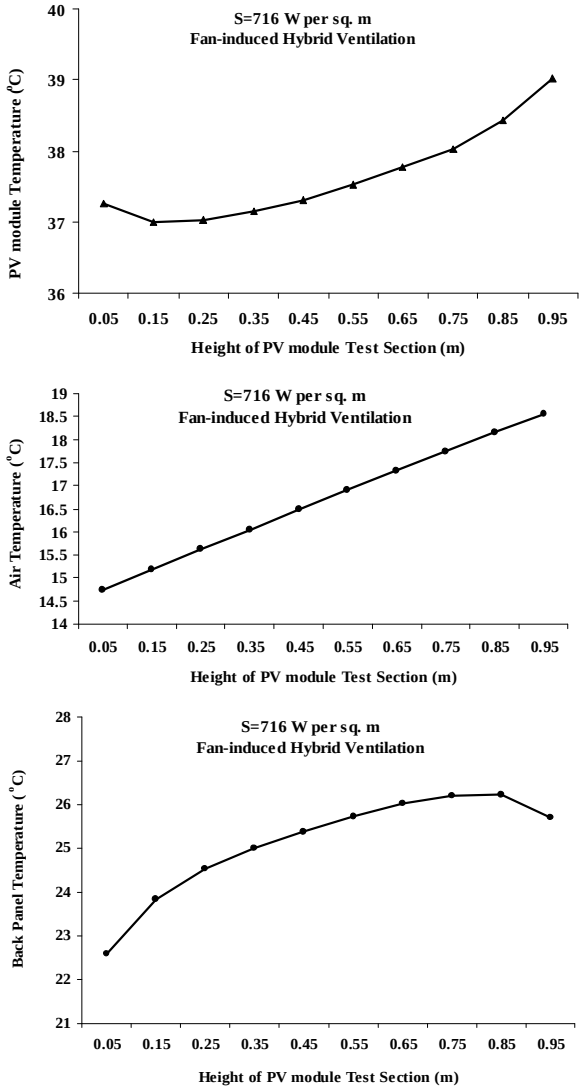

Fig. 5 Temperature plots for PV module, air and back panel with respect to volume of PV module test section

The non-linear temperature plots of PV module and back panel have shown increase in their temperatures with volume or height of PV module test section. The increase in temperature for back panel was observed to be higher than PV module as back panel was heated with radiation heat exchange. Moreover back panel made up of plywood board filled with polystyrene has higher heat storage capacity in comparison to glass coated PV module. Hence, significant cooling of surface of PV module was achieved by radiation heat exchange with back panel. The air temperatures in airflow passage were developed as a function of magnitude of the ambient

air temperature. There was exponential temperature variation of air with height of PV module test section. The maximum convection heat transfer was observed between ambient cold air entering into inlet damper and airflow passage of PV module test section. The dissipation of heat at inlet opening has resulted in considerable increase in temperature of the air. The dissipated heat from the walls of PV modules and back panel was affected by inlet air temperature, as with cold air temperatures increased heat transfer rate has resulted in significantly increasing air temperature at the inlet damper [1]. The heat was transported through the PV module test section was due to convection heat exchange with the air flowing across the cross-sectional area of the test section [1]. The enthalpy change of air was due to thermal capacity rate of air, mc_p, which was inversely proportional to surface temperature of PV module and back panel [1]. The energy balance on a composite control volume (PV module, air and back panel) of 10^{th} node of PV module test section is illustrated in Fig. 6.

The mean air velocity was assumed to be constant in PV module test section for representing nodes of air with same thermal capacity conductances, mc_p also termed as thermal capacity rate C_p through out the height of PV module test section [1]. The amount of dissipated heat from the PV module that has been taken up by air was function of mass flow rate passing over it, thermal capacity of air and temperature difference of air in the airflow passage of PV module test section [1]. The thermal capacity rate mc_p is ventilation heat capacity that was developed for width W across one PV module in the test section [1]. The dissipated heat from the face area (W X H) of PV module test section was transformed into ventilation heat rate across cross-sectional area and eventually was convection heat exchange from the walls due to difference in temperature between the walls and air flowing across cross-sectional area of the solar wall [1].

The validation of the results obtained from the proposed network model and measured values have been conducted [1]. Table 1 has presented comparison of results obtained from the experimental setup and the proposed network model. The results obtained from the model were in good agreement with the measured values. The major cause of deviation of the model from the measured values was due to considerable heating at the inlet damper and heat transfer losses from the side walls of wood and Plexiglas [1].

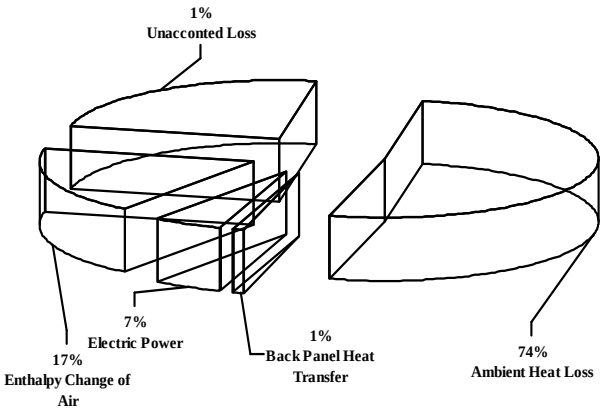

Fig. 6 Energy balance on a composite control volume of 10^{th} node of PV module test section at outlet using enthalpy generation approach

Table 1 Validation results

	Property	Simulated	Observed
Temperature at 10^{th} discretised node (outlet) of PV module test section			
(1)	PV Module	39.2 °C	35.8 °C
(2)	Air	18.6 °C	20.3 °C
(3)	Back panel	25.8 °C	28.9 °C
Temperature difference between 10^{th} air node and 1^{st} air node)			
(4)	Air	3.8 °C	3.0 °C

4 Conclusion

The model has predicted the unknown temperatures at discretised nodes with use of initial conditions of boundary resistive elements. The solution accuracy of the network has been based on the magnitude and number of the connected resistances in the circuit, the smaller the shunt resistance value the greater has been the accuracy.

The network model is a useful tool for accurate prediction of mass flow rate in the electrical analog circuit with voltages at the nodes developed due to wall and air temperatures. The resistive network has been found to be unconditionally stable with algebraic superposition of connected resistive elements in the circuit that were analysed at their maximum electrical analog conductance values under steady state critical operation.

References:

[1] H. Dehra, A numerical and experimental study for generation of electric and thermal power with photovoltaic modules embedded in building façade, submitted/unpublished Ph.D. thesis, *Department of Building, Civil and Environmental Engineering, Concordia University, Montréal, Canada,* August 2004.

Nomenclature:

A	Face area of PV module (m^2)
c_p	Specific heat of air at constant pressure (J $kg^{-1} K^{-1}$)
E_0	Electric power generated by PV module (Watts)
H	Height of PV module test section (m)
h_0	Wind heat transfer coefficient (W $m^{-2} K^{-1}$)
h_{ic}	Convective heat transfer coefficient for PV module (W $m^{-2} K^{-1}$)
h_{jc}	Convective heat transfer coefficient for Back panel (W $m^{-2} K^{-1}$)
hr	Linearized radiation heat transfer coefficient (W $m^{-2} K^{-1}$)
k_{air}	Thermal conductivity of air (Watts $m^{-1} K^{-1}$)
k_i	Thermal conductivity of PV module (Watts $m^{-1} K^{-1}$)
k_j	Thermal conductivity of back panel (Watts $m^{-1} K^{-1}$)
L	Air gap width of channel (m)
m	mass flow rate (for one PV module) through the PV module test section (kg s^{-1})
q	Net heat flux density in PV module (Watts m^{-2})
$Q_{30,1}$	Heat source matrix (30 X 1)
Q(amb)	Ambient heat transfer rate (Watts)
Q(cond)	Conduction heat transfer rate (Watts)
Q(conv)	Convection heat transfer rate (Watts)
Q(enth)	Enthalpy heat transfer rate (Watts)
Q(rad)	Radiation heat transfer rate (Watts)
Q(zone)	Room heat transfer rate (Watts)
S	Absorbed solar radiation by PV module (Watts)
T	Temperature at node (° C).
T_0	Specified ambient air temperature (° C)
$T_{30,1}$	Temperature matrix (30 X 1)
T_i	Temperature of PV module (° C)
T_j	Temperature of Back panel (° C)
T_k	Air temperature in the channel (° C)
T_R	Room air temperature (° C)
U	Conductance at nodal element (Watts)
$U_{30,30}$	Conductance matrix (30 X 30)
v	Air velocity through the channel (m s^{-1})

Subscripts:

i	PV module
j	Back panel
k	Air
o	Ambient air
H	Height of PV module test section
L	Air gap width of airflow passage
R	Room
PV	PV module
W	Width of one PV module